Ocean Sci. Discuss., 8, 1657–1694, 2011
www.ocean-sci-discuss.net/8/1657/2011/
doi:10.5194/osd-8-1657-2011

Ocean Science Discussions

On the export of dense water from the Weddell and Ross Seas

R. Kerr[1,2], K. J. Heywood[3], M. M. Mata[1,2], and C. A. E. Garcia[1]

[1]Laboratório de Estudos dos Oceanos e Clima, Instituto de Oceanografia, Universidade Federal do Rio Grande (FURG), Rio Grande, RS, 96201-900, Brazil
[2]Instituto Nacional de Ciência e Tecnologia da Criosfera (INCT-CRIOSFERA), RS, Brazil
[3]School of Environmental Sciences, University of East Anglia (UEA), Norwich, NR4 7TJ, UK

Received: 21 June 2011 – Accepted: 27 June 2011 – Published: 11 July 2011

Correspondence to: R. Kerr (rodrigokerr@furg.br)

Published by Copernicus Publications on behalf of the European Geosciences Union.

Abstract

We describe the seasonal and interannual variability of volume transports in Weddell and Ross Seas using the 1/12° 20-yr simulation of the OCCAM global ocean general circulation model. The average simulated full-depth cumulative volume transports were 28.5 ± 2.9 Sv ($1\ \mathrm{Sv} \equiv 10^6\ \mathrm{m^3\ s^{-1}}$) and 13.4 ± 5.2 Sv, across the main export regions of the Weddell and Ross Seas, respectively. The values of mean outflow of Antarctic Bottom Water (AABW) (defined by neutral density $\gamma^n \geq 28.27\ \mathrm{kg\ m^{-3}}$) from the Weddell and Ross Seas of 10.6 ± 3.1 Sv and 0.5 ± 0.7 Sv, respectively, agree with the range reported in historical observational studies. Variability in AABW export is predominantly at periods of ~ 1 yr and 2–4 yr. The transit time taken by AABW sourced in the Southern Weddell Sea to reach the main Weddell export zone is ~ 2 yr. Lagged correlation between the thermohaline properties of AABW source waters and AABW export indicates that recent shelf waters freshening trends are likely related to changes in the AABW outflow rates.

1 Introduction

During the IV International Polar Year (IPY; 2007–2009) the scientific community has focused on better understanding the interactions between ocean, atmosphere, and cryosphere, and the role and susceptibility of Polar Regions in a climate change scenario. The *Synoptic Antarctic Shelf-Slope Interactions Study* (SASSI) project (Heywood et al., introductory paper to this special issue) coordinated by the International Antarctic Zone Programme (iAnZone) brought a coordinated international sampling effort around the Antarctic margins (i.e. the zone around the continental shelf-break) during the IPY. The importance of this ocean boundary region between coastal and deep zones is related to dense waters cascading into deep and bottom ocean layers until they reach their density equilibrium in the water column. The densest water that fills the global ocean basins has its main sources in the regional seas around the Antarctic continent and is referred to as Antarctic Bottom Water (AABW) after leaving the source regions (Orsi et al., 1999).

AABW is a mixture of different source water masses with origins both in the coastal and deep ocean regime. Its properties depend on several complex physical coupled ocean-atmosphere-cryosphere processes that occur during its formation, including sea ice growth and brine rejection, opening of coastal polynyas, melting under deep ice shelves, deep convection, and entrainment of overlaying or surrounding waters (Gill, 1973; Carmack and Foster, 1975; Foldvik et al., 1985; Nicholls et al., 2009). The Weddell and Ross Seas (Fig. 1) have broad (~400 km) and deep (~400 m) continental shelves that facilitate some of the processes listed above. AABW is produced at the Antarctic continental margins through mixture of shelf waters near the freezing point (High Salinity Shelf Water – HSSW, and Ice Shelf Water – ISW) with relatively warm and salty intermediate waters (Warm Deep Water – WDW, Modified WDW – MWDW, and Circumpolar Deep Water – CDW, Modified CDW – MCDW). Figure 2 indicates these water masses in the potential temperature-salinity (θ/S) space.

During the last decade several studies have highlighted the variability and trends in the physical properties of AABW source water masses. For example, a long-term trend in salinity revealed freshening of shelf water masses of both the Weddell and Ross Seas (Jacobs et al., 2002; Jacobs and Giulivi, 2010; Hellmer et al., 2011), but the real causes of this freshening are still under debate (e.g., Assmann and Timmermann, 2005; Rignot and Jacobs, 2002). Hellmer et al. (2009) showed that decadal variability of the salinity of the Southwestern Weddell Sea shelf water can be related to the variability of the Southern Annular Mode, which impacts both the ocean circulation dynamics and sea ice processes in the Southern Ocean (Hall and Visbeck, 2002) and, consequently, the AABW contribution to the deep ocean (Kerr et al., 2009a).

At the same time, changes in the intermediate-depth source waters of AABW have also been reported for the last decades. Gille (2002) showed that Southern Ocean waters between 700 m and 1000 m depth had a temperature trend of about +0.01 °C yr^{-1} between the 1950s and 1990s. A similar magnitude of warming (~0.012 °C yr^{-1}) was

OSD
8, 1657–1694, 2011
On the export of dense water from the Weddell and Ross Seas
R. Kerr et al.

reported for the WDW layer inflow to the Weddell Sea during the 1975–2000 period (Robertson et al., 2002). Smedsrud (2005) also reported WDW warming near the Greenwich Meridian from 1977 to 2001, while Fahrbach et al. (2004) showed evidence that this approximately 40-yr warming period could be finishing after 1998. Alternating periods of WDW cooling and warming were already reported by Gordon (1982) during the 1970s.

The changes in AABW source water masses are impacting the properties of the recently ventilated deep and bottom waters formed around the Antarctic continent (e.g., Aoki et al., 2005; Johnson, 2009; Ozaki et al., 2009). Kerr et al. (2009a) revealed that Weddell Sea Bottom Water (WSBW) contribution to the total water mass mixture in the Weddell Basin exhibited a decreasing contribution of ∼20 % between the 1980s and the 1990s both near the Greenwich Meridian (1984–1998) and in the World Ocean Circulation Experiment (WOCE) SR4 repeat section (Fahrbach et al., 2004) near the tip of the Antarctic Peninsula (1989–1998). Aoki et al. (2005) indicated that bottom waters in the Antarctic-Australian Basin are becoming cooler (∼0.2 °C) and fresher (∼0.03) over a 1994 to 2003 period. More recently, Rintoul (2007) highlights a faster AABW freshening between 1995 and 2005 than that observed between the late 1960s and the 1990s.

Our present study aims to better understand the variability of AABW export and how the variability of AABW source water masses is influencing deep and bottom water export. Here we focus our investigation on comparing the results from the Weddell and Ross Seas, two of the main areas of AABW production (Orsi et al., 1999). It is well known that synoptic and almost uninterrupted properties over a long time period and throughout all seasons are required to perform time series analyses. However historical observed subsurface Southern Ocean databases lack long historical records, are seasonally biased and suffer from scarcity of data in some areas of difficult access due to environmental conditions and/or logistic operations, therefore modelling results are an alternative way to study the impact of source water variability on AABW export. Based on this assumption, we based our work on the output from the high spatial

OSD
8, 1657–1694, 2011

Title Page
Abstract | Introduction
Conclusions | References
Tables | Figures
◀◀ | ▶▶
◀ | ▶
Back | Close
Full Screen / Esc
Printer-friendly Version
Interactive Discussion

resolution 1/12° global eddy-resolving version of the Ocean Circulation and Climate Advanced Modelling (OCCAM) model (Coward and de Cuevas, 2005).

The paper is organized as follows: the ocean model characteristics and forcing fields are briefly described in the next section. Section 3 shows the characteristics of the continental shelf cross-sections and the model hydrographic properties. Section 4 discusses the cross-section volume transport variability along the continental margins. Section 5 presents the main results and discussion associated with source water mass variability and bottom water in the deep ocean. The main conclusions are summarized in Sect. 6.

2 Model description and forcing

Kerr et al. (2009b) showed the deficiencies and difficulties in simulating Southern Ocean deep water masses in the oceanic component of the National Center for Atmospheric Research-Community Climate System Model (NCAR-CCSM) suggesting that they are mainly due to the absence of some coupled cryosphere-ocean processes. Renner et al. (2009) highlighted that the choice of the model must be made carefully and according to the purpose of the study, and they also demonstrated that OCCAM 1/12° simulation is a good choice to perform analyses regarding deep water masses.

OCCAM is a global ocean general circulation model (OGCM) (Coward and de Cuevas, 2005) coupled with a dynamic-thermodynamic sea ice model (Aksenov, 2002), which is essential to better represent the AABW properties because both dynamic and thermodynamic processes play significant roles in the Southern Ocean climate variability and bottom water formation process (Jacobs and Comiso, 1989; Venegas and Drinkwater, 2001). However, ice shelves, icebergs and ice sheet runoff are not included explicitly in the model. The model has 66 levels in the vertical, whose thickness increases approximately from 5 m at the surface to 205 m for the deepest layer. The bathymetry is constructed from Smith and Sandwell (1997) and Digital Bathymetry Database 5 (DBDB5, 1983).

OSD
8, 1657–1694, 2011

The OCCAM model was run at the National Oceanographic Centre, Southampton, UK. In this work we use the monthly output from the OCCAM 1/12° simulation called "run 401" (Coward and de Cuevas, 2005), which was extracted from the OCCAM data selector website (http://www.noc.soton.ac.uk/JRD/OCCAM/EMODS/). The output variables used in this work are potential temperature, salinity, and zonal and meridional velocity. The run was forced using 6-hourly winds and heat fluxes from the National Centers for Environmental Prediction (NCEP) reanalysis data (Kalnay et al., 1996; Large et al., 1997) and was initialized using WOCE climatology (Gouretski and Jancke, 1996) for potential temperature and salinity with additional data for the Arctic Ocean. Sea ice in the Southern Ocean was set to 1.50 m thickness of sea ice and 0.15 m snow in all cells south of 65.25° S with an ice concentration of 99 % in each affected grid cell. The simulation ran for 20 yr spanning from 1985 to 2004, although our analysis excludes the first 4 yr because this period includes the model spin-up phase. A detailed assessment of the OCCAM 1/12° simulation (hereafter referred to as OCCAM only) regarding the representation of physical properties in the Weddell Sea was discussed by Renner et al. (2009). Here we extend their analysis by providing a validation of the model bottom water export time series. Hereafter the reader is directed to Fig. 1 for all regional oceanic and topographic locations cited in the text.

3 Southern Ocean representation

3.1 Modelled hydrographic sections

A total of four continental shelf and slope cross-sections (for locations see Fig. 1) were selected in the Weddell and Ross Seas to investigate the AABW response to shelf and intermediate-depth source water variability. These sections were chosen following the work of Baines and Condie (1998), which showed them to be sites of AABW downslope flow, and also because of the availability of historical data nearby. In the Weddell Sea the sections are defined as: (i) the main outflow route of bottom water

OSD
8, 1657–1694, 2011

export (Naveira Garabato et al., 2002; Franco et al., 2007), coincident with the western part of the WOCE SR4 repeat section (Fahrbach et al., 2004), and (ii) the southern continental shelf near the Filchner-Ronne Ice Shelf zone that is known as a region of AABW production (Foldvik et al., 1985; Nicholls et al., 2009). In the Ross Sea the sections are chosen to be: (i) the bottom water outflow area near Cape Adare, which is an area intensively studied through the US Cross-Slope Exchanges at the Antarctic Slope Front (AnSlope) and the Italian Climatic Long-term Interaction for the Mass balance in Antarctica (CLIMA) programs (Gordon et al., 2009), and (ii) close to the west branch of the Ross Sea cyclonic gyre that is indicated as an export area of the less dense variety of Ross Sea Bottom Water (RSBW; Ozaki et al., 2009). These four sections can represent the AABW export (hereafter referred to as export sections) and formation (hereafter referred to as formation sections) zones in both the Weddell and Ross Seas. All sections spanned from ~500 m to 4000 m deep, except for the Ross Sea export section that is interrupted at 3000 m because of the complex bathymetry surrounding the area.

Figure 2 shows a comparison between observed and simulated θ/S diagrams of each section that are simulated by the model. The observed thermohaline values were obtained from the World Ocean Database 2005 (Boyer et al., 2006). In order to increase the number of observations, we also selected all Conductivity-Temperature-Depth (CTD) hydrographic data within an area of 2° longitude (~100 km for Weddell Sea export section and ~70 km for all others sections) from both east and west of each section. Although ice shelf processes are not considered in OCCAM, which is evidenced by the lack of ISW representation in the model, the water masses on the continental shelf are represented reasonably well in the sections (Fig. 2). Intermediate waters, with neutral density (γ^n; Jackett and McDougall, 1997) between 28.0 kg m^{-3} and 28.27 kg m^{-3}, are warmer and saltier than observations by ~0.5 °C and ~0.03, respectively, in all sections. Despite the slight differences in θ and S absolute values, the model shows a good representation of water masses in the Weddell and Ross Seas continental margins, as earlier reported for the Northwestern Weddell Sea by

Renner et al. (2009). We conclude that OCCAM preserves the observed general θ/S shape but it also represents the pattern of water mass structure for both coastal and open ocean regimes in the Antarctic continental margins (Fig. 2), which provides a high degree of confidence in the analysis of the model time series.

3.2 AABW source layers depth

Two depth ranges were chosen from the OCCAM model to represent the AABW source water masses. We represent the shelf/surface layer (SL), as an average of the 4 model levels between 100 m and 150 m (levels 15–18), while for the intermediate layer (IL) the 4 model levels were averaged between 400 m and 600 m (levels 28–31). The SL defined here encompasses both the shelf water masses in the Antarctic coastal regime and the mixture of waters at the continental slope, such as MWDW in the Weddell Sea that is an important source for AABW formation (Foster and Carmack, 1977). In the oceanic regime, the SL represents the Antarctic surface water masses. The IL encompasses the densest shelf waters present on the broad western and southwestern continental shelves as well as the cores of intermediate-depth source water that reach the continental slope (e.g. WDW θ_{max} is found around 500 m in the Weddell Sea; Orsi et al., 1993).

Averaged fields of potential temperature and salinity in the SL and IL layers are presented in Fig. 3 for the entire OCCAM period (1988–2004). The SL temperature is around $-1.5\,^{\circ}$C in both deep ocean and coastal regimes (Fig. 3a), characterizing the Winter Water in the oceanic waters (i.e. a remnant of the deep winter mixed layer) and the shelf waters, respectively. The temperature slightly increases to $\sim 0\,^{\circ}$C along the continental margin of the Weddell and Ross Seas (Fig. 3a), caused by mixing of shelf waters with upwelled intermediate waters (i.e. WDW or CDW) onto the shelves. Typical high salinity values of the Weddell and Ross Seas shelf waters are observed in the Antarctic coastal regime of the model. The highest salinity plume of water from the Ross Sea western continental shelf is advected westward until $\sim 90^{\circ}$ E in the Davis Sea. CDW upwelling also contributes to the high salinity values simulated in the Western

OSD
8, 1657–1694, 2011

On the export of dense water from the Weddell and Ross Seas

R. Kerr et al.

Pacific Ocean sector (Fig. 3b). The increasing influence of mixing with WDW is noted in the Weddell Sea with increase in salinity values from ~ 20° E to near the coast of Enderby Land, following the Weddell Gyre circulation (Fig. 3b).

Values of θ in the IL ($< -1.5\,^{\circ}$C) are around surface freezing point near the Antarctic coast (Fig. 3c), slightly increasing offshore to ~ 0 °C. In open ocean areas, relatively warm CDW ($> 1\,^{\circ}$C) is seen in the Indian, Western Pacific, Ross, and Bellingshausen and Amundsen (B&A) sectors (Fig. 1). In the Weddell Sea, CDW cools through mixing with surrounding cooler waters as it enters in the Weddell Gyre, marked by WDW temperatures between 0 °C and 0.5 °C (Fig. 3c). The salinity field depicted in Fig. 3d shows most clearly the influence of CDW or WDW within the Ross and Weddell Seas. The model potential temperature and salinity fields at AABW source layers reveal that Weddell Sea SL and IL waters are saltier and colder in oceanic regime, respectively, than in the Ross Sea, as has been noted previously by Orsi and Whitworth (2007).

4 Cross-section volume transport

4.1 Full-depth volume transport

The mean full-depth volume transports, and their respective standard deviations, for the Weddell and Ross Sea export sections during the 17-yr period of OCCAM simulation are respectively 28.5 ± 2.9 Sv (1 Sv $\equiv 10^6\,\text{m}^3\,\text{s}^{-1}$) and 13.4 ± 5.2 Sv, while for the formation sections the values are respectively 21.3 ± 3.6 Sv and 18.4 ± 2.3 Sv (Fig. 4). Positive transports denote northward/eastward. The error estimates quoted are the standard deviations of the monthly values over the 17-yr model run. The gyre transports at the two locations are not the same because the sections as shown do not include the whole of the Weddell/Ross Gyre transports. The OCCAM simulated transports are reasonable compared with summer-time observations and moored short time series for both Weddell (e.g., Fahrbach et al., 1994; Muench and Gordon, 1995; Naveira Garabato et al., 2002) and Ross Seas (e.g., Reid, 1997; Chu and Fan, 2007).

OSD
8, 1657–1694, 2011

On the export of dense water from the Weddell and Ross Seas

R. Kerr et al.

On the other hand, the Weddell Gyre transport is somewhat lower than the value of 46 ± 8 Sv estimated in summer 2007 (Thompson and Heywood, 2008). This transport was calculated with in situ data from the *Antarctic Drift Experiment Link to Isobaths and Ecosystems* (ADELIE) project, which resolved the frontal current system more accurately than the previous studies using a high-resolution hydrography and Lowered Acoustic Deep Current Profiler (LADCP) survey. Nevertheless, the OCCAM model transports represents an average over 17-yr period and one might expect them to be less than some observed values from snapshot cruises or short time series (< 3 yr), which are subject to short-term variability and/or long-term trends.

4.2 Bottom layer definition

In this study we do not attempt to distinguish between the regional differences of deep and bottom water masses around the Southern Ocean, since we wish to use a consistent definition for all regions. Hereafter, we define the *bottom layer* as the part of the water column denser than γ^n of 28.27 kg m^{-3}, in accordance with the definition of AABW given by Orsi et al. (1999). This layer encloses all AABW regional varieties in the Southern Ocean despite the differences in their physical properties in each source area (Whitworth et al., 1998). In fact, the bottom layer as defined here encloses the entire deep and bottom water mass with θ lower than 0 °C in the continental slope and deep ocean regime. Moreover, OCCAM model reproduces well these bottom layer waters around the Antarctic margins. This can be clearly seen in OCCAM fields for the Weddell Sea export section (Fig. 5), where the September climatology is given as an example of the typical water mass structure.

4.3 Bottom layer volume transport

The average bottom layer cumulative volume transports in OCCAM for Weddell and Ross Sea export sections are 10.6 ± 3.1 Sv and 0.5 ± 0.7 Sv respectively, while the formation sections transports are 3.1 ± 0.9 Sv and 0.5 ± 0.4 Sv, respectively (Fig. 6).

OSD
8, 1657–1694, 2011

To assess whether the bottom volume transport time series are realistic, we compare the bottom layer volume transport simulated by OCCAM in the Weddell Sea export section with previous observational studies in the same area carried out by Fahrbach et al. (1995) and Fahrbach et al. (2001), hereafter referred to as F95 and F01, respectively.

The periods covered by the F95 and F01 analyses span between 1989–1993 and 1989–1998, respectively, and they are included in the OCCAM simulated period. The absolute values (not shown) of both observational and modelled bottom volume transport differ along the years, mainly because we used different bottom layer definitions in this work (i.e. including both AABW varieties found in the Weddell Sea), however the two time series follow the same pattern. In this context, the values shown in Fig. 7 are normalized and represent the number of standard deviations from the overall mean to allow model-observation comparison. Figure 7 shows that the normalized OCCAM simulated bottom volume transport fits well with the observational studies both on interannual (Fig. 7a; $r = 0.53$; $p = 0.10$; $N = 10$) and monthly cycles (Fig. 7b; $r = 0.40$; $p = 0.05$; $N = 36$). In addition, the observed and modelled annual standardized mean current velocity for the bottom layer show similar patterns (Fig. 7c) during the F01 observational period, with mean absolute bottom current velocity of $4.0 \pm 0.89\,\mathrm{cm\,s^{-1}}$ (OCCAM) and $3.45 \pm 0.58\,\mathrm{cm\,s^{-1}}$ (F01; see their Fig. 12a).

In general, the mean bottom water export rates from Weddell and Ross Seas are well supported by observations. The OCCAM mean bottom layer transport of ~ 11 Sv for the Weddell export section (Fig. 6a) is near the values of Weddell Sea Deep Water (WSDW) export of 6.7 ± 1.0 Sv and ~ 9 Sv obtained, respectively, by Naveira Garabato et al. (2002) over the South Scotia Ridge from LADCP data and by Franco et al. (2007) through an application of a box inverse method in the main passages of the South Scotia Ridge. In the Ross Sea, Whitworth and Orsi (2006) reported a transport of water colder than 0 °C of 1.95 ± 1.85 Sv near the shelf break off Cape Adare. The mean bottom layer transports of 0.5 ± 0.7 Sv and 0.5 ± 0.4 Sv simulated by the OCCAM model, respectively from the Ross Sea export and formation section (Fig. 6c and d), are slightly lower than the observed values, but their values are within the range of recent observations in the area cited above.

The simulated seasonal cycles of both standardized export and formation transports sections for the Weddell Sea show a similar pattern through the year, with the former showing the maximum volume transport lagging the latter by ∼ 1 month (Fig. 8a). For the export section, the maximum and minimum monthly mean transport of 12.2 ± 3.0 Sv and 8.6 ± 2.8 Sv were observed during June and January, respectively. For the formation section, the maximum and minimum monthly mean transport of 4.0 ± 0.9 Sv and 2.2±0.5 Sv occurred during May and January, respectively. Note that the values quoted above are actual values simulated by the model and not the values normalized by the monthly mean and standard deviation values as shown in Fig. 8. In this case, the normalization procedure was needed because of the difference in magnitude of volume transports in the export and formation sections (Fig. 6). Thus, the monthly mean transports of bottom water in the Weddell Sea are maximum and minimum respectively during early austral winter and summer seasons, corroborating with the results of F95 that conclude the AABW outflow is subject to a seasonal cycle with minimum temperatures and maximum velocities in early austral winter. In the Weddell Sea export zone there is an insignificant delay of approximately one month in the model seasonal cycle (Fig. 8a) when compared with the results reported by F01, which showed maximum and minimum transport in May and December.

In contrast, the seasonal cycles of standardized bottom volume transport in the Ross Sea (Fig. 8b) for the export and formation sections present higher variability than in the Weddell Sea. The Ross Sea export zone show a maximum and minimum absolute monthly mean transport of 1.0 ± 1.1 Sv and 0.06 ± 0.1 Sv occurring during June and December, respectively, the same months as in the Weddell Sea. Inside the Ross Sea the formation section shows a semi-annual cycle with maxima in March–May and July–September and minima in June–July and December. The maximum and minimum monthly mean transports of 0.7 ± 0.5 Sv and 0.1 ± 0.3 Sv occurred in May and December, respectively. Semi-annual cycles in current measurements and circulation

OSD
8, 1657–1694, 2011

strength have also been observed in the Ross Gyre domain, as highlighted by Assmann et al. (2003) and references cited therein. There were no significant differences in the seasonal cycle of bottom layer volume transport from alternative sections selected to the south and to the east in the Weddell Sea and to the west and to the east in the Ross Sea of the export and formation sections, respectively (Fig. 8). These results support the robustness of the location chosen to represent the whole regional area.

Wavelet analysis of the detrended bottom water monthly volume transport time series reveals both the dominant modes of bottom water export variability and how those modes vary in time (Fig. 9). In general, the dominant period of variability is 1 yr due to seasonal changes in the wind-driven gyres. However, the annual cycle is absent up to 1995 (see also Fig. 6c) for the Ross Sea export section, while in the Weddell Sea the annual cycle is significant through the whole time of the simulation. The wavelet analysis also highlights a significant periodicity at 2–4 yr for the export section (Fig. 9a) in the Weddell Sea. For the Ross Sea formation section (not shown) low energy is associated with the variability of bottom water export. Venegas and Drinkwater (2001) found that interannual variability of sea ice concentration, sea ice drift and sea level pressure presented a 3–4 yr period in the Weddell Sea. They also pointed out that sea ice variability spanning from 1979 to 1998 appears to be associated with a change in the shape and characteristics of the Weddell Gyre circulation around the 1990s. Our findings are in consonance with the dominant period of AABW export variability in this region (Fig. 9).

It is difficult to isolate which processes of the Earth's climate system are acting to reduce or increase the bottom water export from the Antarctic source areas. Both polar and extrapolar climate variability (e.g., see McKee et al., 2011) over a broad range of spatial and temporal scales are likely interacting to affect AABW production and export from the Antarctic shelves. Next we explore how changes in AABW source water masses can be associated with variability of bottom water export from Antarctic regional seas.

Discussion Paper | Discussion Paper | Discussion Paper | Discussion Paper |

OSD

8, 1657–1694, 2011

On the export of dense water from the Weddell and Ross Seas

R. Kerr et al.

5 Correlations between AABW sources properties and deep ocean export

Cross-correlation maps between the anomaly time series of both the bottom water volume transport (see Sect. 4.3) and the properties of the AABW source layers (see Sect. 3.2) were constructed for the four selected model sections. Prior to the analyses, a linear trend was removed from each time series because such trends are likely to be due to model drift. Moreover, the seasonal cycle was removed from each time series to allow us to see the underlying variability (see Sect. 4.3). The seasonal cycle was removed from all time series by subtracting monthly means from the data and finally, we filtered all time series with a Butterworth filter with a 12-month window to further smooth the deseasoned time series. In order to see the robustness of the results obtained, sensitivity analysis (not shown) was performed on different selected SL and IL from the OCCAM model, but changes in the correlation patterns were not significant.

We expect cold and salty shelf waters to be positively correlated with bottom water export at some lag, because our hypothesis is that enough brine is rejected into the lower layers during coastal sea ice formation to make dense shelf waters more abundant over the shelf, which would lead to a greater amount of those dense waters spilling off the continental shelf and thus intensifying AABW formation. The bottom volume transport in the Weddell Sea export section is significantly correlated ($r \geq 0.7$, $p < 0.05$, $N = 204$) with SL salinity in the Western and Southern Weddell Sea continental shelf (Figs. 10 and 11). All cross-correlations presented highest values at lag-0. A spatial pattern can be clearly seen with positive cross-correlations in the shelf regime all around the continent, and negative cross-correlations in the open ocean (Fig. 11c). We conclude that the Weddell Sea bottom water outflow and circumpolar thermohaline shelf water properties co-vary (Fig. 11).

The above findings are striking because one would expect the SL waters to take a while to reach the export region. Assuming the OCCAM mean AABW velocities for the whole simulated period to be $4\,\mathrm{cm\,s^{-1}}$ and $1.2\,\mathrm{cm\,s^{-1}}$ for Weddell export and formation sections, respectively, and a total distance between those sections of about

OSD
8, 1657–1694, 2011

1515 km, AABW sourced in the Southern Weddell Sea will take approximately 1.8 yr to reach the export region. Thus, the high positive correlations between shelf water salinity and bottom water export cannot be taken as cause-consequence but instead they are co-varying in time, probably because both are associated with faster or slower phases of the wind-driven Weddell Gyre.

In fact, the high correlation between the AABW outflow and the shelf regime practically disappears when the time series are lagged up to a period of 5 yr (volume transport lagging water mass properties; Fig. 12c). The time interval of 5 yr is consistent with the shelf water residence time of ~6 yr reported in the Weddell Sea (Schlosser et al., 1991; Mensch et al., 1998). At this lag, shelf water properties are anti-correlated ($r \le -0.7$; $p < 0.05$; $N = 204$) with bottom water transport at the export section. Positive high correlations between bottom water transport and SL salinity are found along both the Western and Southern Weddell Sea continental slope and in the CDW inflow region around 20° W (Fig. 12c). The θ field presents a similar pattern of correlation but not as well defined (Figs. 11a and 12a), thus highlighting that the wind is just driving both the AABW source properties variability and AABW export. Finally, another positive feedback on the above process could result from an increasing vertical mixing on the shelf if a stronger wind spins up the Weddell Gyre.

The correlation maps between SL thermohaline properties and the bottom water transport at export section in the Ross Sea (not shown) showed similar patterns to those of the Weddell Sea (Fig. 11a and c). However, the correlations are slightly lower and not completely circumpolar as calculated for the Weddell Sea. In contrast to the Weddell Sea, AABW with sources within the Ross Gyre will take only 6.5 months to reach the export region near Cape Adare, assuming mean AABW velocities for the whole OCCAM period to be 5.3 cm s^{-1} and 0.7 cm s^{-1} respectively for the Ross Sea export and formation sections, and a total distance between them of 515 km. The residence time of ~4 yr for Ross Sea shelf waters (Trumbore et al., 1991) suggests that it may take several years for the thermohaline variability in shelf water to affect bottom water export.

OSD
8, 1657–1694, 2011

Correlations between bottom water export and production transport time series of both Weddell and Ross Seas reach their maximum ($r = 0.5$; $p < 0.05$; $N = 204$) at 4.6 yr, which is longer than the calculated transit time for the Weddell (1.8 yr) and Ross Seas (6.5 months). In fact, AABW export from those areas has significant contributions from the Northwestern Weddell Sea continental shelf bordering the eastern margins of the Antarctic Peninsula (Huhn et al. 2008) and the southwestern area in the vicinity of the Ross Ice Shelf (Whitworth and Orsi 2006). In this context, the time series of bottom water sourced in the Northwestern Weddell Sea (see Fig. 1) and exported from the Weddell Sea export section are highly correlated ($r = 0.8$; $p < 0.05$; $N = 204$) with a time lag of 1 yr, a period consistent with the shelf water residence time in this region (e.g., Hellmer et al., 2011). Thus, the correlation maps are probably suggesting that recent shelf water freshening trends (e.g., Jacobs and Giulivi, 2010; Hellmer et al., 2011) will decrease the rate of AABW export in a relatively short period (< 5 yr), regardless of the cause of that freshening (e.g. more precipitation, retreat of sea ice boundary, ice shelf disintegration).

The correlation maps between bottom water export and θ and salinity time series, at intermediate-depth layer, are slightly different from each other (Fig. 11b and d). AABW outflow from the Weddell Sea is correlated ($r \geq 0.5$; $p < 0.05$; $N = 204$) at lag-0 with WDW thermohaline properties entering and following the Weddell gyre circulation. Significant correlations ($r \geq 0.7$; $p < 0.05$; $N = 204$) are found with intermediate-depth waters at the Western Weddell Sea continental slope. In general, bottom water export from the Weddell Sea is significantly correlated with both CDW and WDW characteristics. Moreover, high correlation is observed with salinity variability in the deepest areas of the western and southern continental shelves (i.e. densest shelf water variety) of both the Weddell and Ross Seas (Fig. 11d). Once more, correlation at lag-0 must be due to changes in both the export and the water mass properties being driven by the wind field. Unlike the cross-correlation maps for the SL, the strongest correlations at lag-0 (Fig. 11b and d) are maintained in some areas of the IL map at lag-5, such as the Western and Southern Weddell Sea continental margins (Fig. 12b and d). In fact, 5 yr

OSD
8, 1657–1694, 2011

is approximately the residence time of the waters (∼6 yr; Hoppema et al., 2010) in the Weddell Gyre. Dellnitz et al. (2009) through numerical simulation found that the Weddell Gyre surface and bottom water residence times vary between 1 and 5 yr, while the residence time for intermediate-depth water varies seasonally with periods between 5 and 12 yr.

Similar patterns of correlations appear for the IL for both the Weddell (Fig. 11b and d) and Ross Seas export sections (not shown). In the Ross Sea, the pattern is characterized by positive correlations with CDW properties along the cyclonic gyre circulation and with IL salinity (depth of ∼500 m) in the Ross Sea coastal regime. However, in the Ross Sea the influence of CDW salinity characterized by positive correlations along the gyre circulation is not as clear at lag-0 as in the Weddell Sea (Fig. 11d), but instead correlation becomes higher as the time series are lagged up to 5 yr (Fig. 12d).

We have shown that AABW export co-varies with temperature and salinity of SL and IL at lag-0, implying that they are both responding to the same forcing, which is likely to be changes in the wind-driven cyclonic gyre circulation. The model results point out that the observed variability of shelf waters properties, such as the recent freshening trends reported, might be a proxy for changes in volume transport of newly-exported AABW from its source areas within a short time (i.e. a time less than the shelf water residence period on the continental shelf). Fresher shelf waters in OCCAM are associated with reductions in AABW export.

Finally, using mooring observations, Gordon et al. (2010) showed the absence of the AABW cold pulse in the Northern Weddell Sea during the year 2000. During that time, the OCCAM simulation points to a decreasing AABW volume transport anomaly from 1998 onwards and those anomalies remain negative in the Southern Weddell Sea until 2004, at least (Fig. 13c). Similar negative values of volume transport anomaly is observed during this year in the Northwestern Weddell Sea AABW formation zone (Fig. 13b), which decrease the volume of AABW export from the Weddell Sea (Fig. 13a). Furthermore, the AABW negative volume transport anomalies probably result from the reduction of the AABW production in the Weddell Sea, which, in turn,

OSD
8, 1657–1694, 2011

On the export of dense water from the Weddell and Ross Seas

R. Kerr et al.

should be related with density changes of the newly-formed AABW (i.e. less dense varieties; Fig. 14). Therefore, the lack of newly-formed dense AABW variety during the beginning of 2000's could also be linked to the absence of the AABW cold pulse as reported by Gordon et al. (2010).

6 Conclusions

In this study, we have shown that averaged AABW (i.e. $\gamma^n \geq 28.27\,\mathrm{kg\,m^{-3}}$) outflow is ~ 11 Sv in the Northwestern Weddell Sea and only ~ 1 Sv in the Ross Sea. In the bottom water formation regions, bottom water transports of ~ 3 Sv and ~ 0.5 Sv were estimated in the Weddell and Ross Seas, respectively. Those rates of AABW export from both regions are in good agreement with previous observed studies. The AABW export varies mainly at 1 yr and 2–4 yr time scales. In the Weddell Sea, the 2–4 yr period is consistent with time scale changes in the atmosphere, sea ice, and ocean surface (Venegas and Drinkwater, 2001), which are directly linked to the processes of AABW formation.

AABW export co-varies with AABW source water masses thermohaline properties at lag-0, suggesting that they are both responding to the same physical forcing, such as the wind patterns driving cyclonic gyre circulation. The recent freshening trends reported for shelf water masses (sources of AABW) in the Southern Ocean may be used to determine changes in the volume transport of newly-formed AABW cascading down the slope, as suggested through saltier shelf water leading to greater volume of AABW export. However, the results cannot be interpreted as cause-consequence, implying that more efforts must be directed to better understanding the role of the freshening and/or warming trends of AABW sources on changes in AABW production and export to the global oceans.

Additionally, AABW with sources in the Southern Weddell Sea will take ~ 2 yr to reach the main export region along the South Scotia Ridge. Thus, those source waters are subject to transformation through mixing with other regional varieties along the

OSD
8, 1657–1694, 2011

path. Furthermore, changes in the thermohaline properties of newly-formed AABW may eventually influence the characteristics of the waters being exported from the Weddell Sea. That is supported by the results presented in Fig. 14, which unveil the same temporal signal in the neutral density anomalies time series from the Southern to the Northern Weddell Sea.

Assimilation products, such as the Simple Ocean Data Assimilation reanalysis, have been recently designated to improve the representation of Southern Ocean bottom waters (Kerr et al., 2011), where models sometimes are deficient to represent them (Kerr et al., 2009a). The inclusion of ice shelf processes and other cryosphere components would certainly improve the representation of the water mass in shelf break zone in future simulations, providing a better representation of bottom water properties cascading down the slope to the deep sea.

Finally, observational studies focusing on long-term records (and also longer models simulations) of both AABW export and thermohaline properties have to be continued in key areas of AABW outflow, such as the northwestern region of Weddell and Ross Seas investigated here, but also the region around the Kerguelen plateau in the Davis Sea as recently indicated by Fukamachi et al. (2010). Models such as OCCAM are useful to increase our understanding of the role of AABW regional outflows in the global climate system.

Acknowledgements. This study is a contribution to International Polar Year – SASSI (UK) and SOS-CLIMATE (Brazil) projects through the activities of the Brazilian High Latitudes Oceanography Group (GOAL) in the Brazilian Antarctic Program (PROANTAR). GOAL has been funded by the Brazilian Ministry of Environmental (MMA), the Brazilian Ministry of Science and Technology (MCT), and the Council for Research and Scientific Development of Brazil (CNPq; 550370/2002-1; 520189/2006-0). The authors also thank the Brazilian National Institute of Science and Technology of Cryosphere (INCT-CRIOSFERA; 573720/2008-8). R. Kerr acknowledges financial supports received from POGO-SCOR Fellowship Program, CNPq PhD Split Fellowship Program (SWE – 201843/2008-0), and CAPES Foundation.

References

Aksenov, Y.: The sea ice-ocean global coupled ARCICE project report – Part 1: Description of dynamical-thermodynamical sea ice model. SOC research and Consultancy Report, 83 pp., Southampton Oceanography Centre, 2002.

Aoki, S., Rintoul, S. R., Ushio, S., Watanab, S. and Bindoff, N. L.: Freshening of the Adelie Land Bottom Water near 140° E. Geophys. Res. Lett., 32, L23601, doi:101029/2005GL024246, 2005.

Assmann, K. M. and Timmermann, R.: Variability of dense water formation in the Ross Sea, Ocean Dynam., 55, 68–87, doi:10.1007/s10236-004-0106-7, 2005.

Assmann, K. M., Hellmer, H. H., and Beckmann, A.: Seasonal variation in circulation and water mass distribution on the Ross Sea continental shelf. Antarct. Sci., 15(1), 3–11, doi:10.1017/S0954102003001007, 2003.

Baines, P. G. and Condie, S.: Observations and modelling of Antarctic downslope flows: A review, in: Ocean, Ice, and Atmosphere: Interactions at the Antarctic Continental Margin, edited by: Jacobs, S. S. and Weiss, R. F., Antarctic Research Series, 75, Washington DC: AGU, 29–49, 1998.

Boyer, T. P., Antonov, J. I., Garcia, H. E., Johnson, D. R., Locarnini, R. A., Mishonov, A. V., Pitcher, M. T., Baranova, O. K., and Smolyar, I. V.: World Ocean Database 2005, in: NOAA Atlas NESDIS 60, edited by: Levitus, S., US Government Printing Office, Washington, D.C., 190 pp., 2006.

Carmack, E. C. and Foster, T. D.: On the flow of water out of the Weddell Sea. Deep-Sea Res., 22, 711–724, 1975.

Chu, P. C. and Fan, C.: An inverse model for calculation of global volume transport from wind and hydrographic data, J. Marine Syst., 65, 376–399, 2007.

Coward, C. A. and de Cuevas, B. A.: The OCCAM 66 Level Model: physics, initial conditions and external forcing, Tech. Rep. SOC Internal Report, No. 99, Southampton Oceanography Centre, 2005.

DBDB5: US Naval Oceanographic Office, and the US Naval Ocean Research and Development Activity, Digital bathymetric Data Base-5 minute grid, 1983.

Dellnitz, M., Froyland, G., Horenkamp, C., Padberg-Gehle, K., and Sen Gupta, A.: Seasonal variability of the subpolar gyres in the Southern Ocean: a numerical investigation based on transfer operators, Nonlinear Proc. Geoph., 16, 655–664, 2009.

Fahrbach, E., Rohardt, G., Schröder, M., and Strass, V.: Transport and structure of the Weddell Gyre, Ann. Geophys., 12, 840–855, doi:10.1007/s00585-994-0840-7, 1994.
Fahrbach, E., Rohardt, G., Scheele, N., Schröder, M., Strass, V., and Wisotzki, A.: Formation and discharge of deep and bottom water in the Northwestern Weddell Sea, J. Mar. Res., 53(4), 515–538, 1995.
Fahrbach, E., Harms, S., Rohardt, G., Schröder, M., and Woodgate, R. A.: Flow of bottom water in the Northwestern Weddell Sea, J. Geophys. Res., 106(C5), 2761–2778, 2001.
Fahrbach, E., Hoppema, M., Rohardt, G., Schröder, M., and Wisotzki, A.: Decadal-scale variations of water mass properties in the deep Weddell Sea, Ocean Dynam., 54, 77–91, 2004.
Foldvik, A., Gammelsröd, T., and Törresen, T.: Circulation and water masses on the Southern Weddell Sea shelf, in: Oceanology of the Antarctic Continental Shelf, edited by: Jacobs, S. S. and Weiss, R. F., Antarctic Research Series, 43, Washington DC, AGU, 5–20, 1985.
Foster, T. D. and Carmack, E. C.: Antarctic bottom water formation in the Weddell Sea, in: Polar oceans, edited by: Dunbar, M. J., Montreal, Arctic Institute of North America, 167–177, 1977.
Franco, B. C., Mata, M. M., Piola, A., and Garcia, C. A. E.: Northwestern Weddell Sea deep outflow into the Scotia Sea during the austral summers of 2000 and 2001 estimated by inverse methods. Deep-Sea Res. Pt. I, 54, 1815–1840, 2007.
Fukamachi, Y., Rintoul, S. R., Church, J. A., Aoki, S., Sokolov, S., Rosenberg, M. A., and Wakatsuchi, M.: Strong export of Antarctic BottomWater east of the Kerguelen plateau, Nat. Geosci., 3, 327–331, doi:10.1038/NGEO842, 2010.
Gill, A. E.: Circulation and bottom water production in the Weddell Sea, Deep-Sea Res., 20, 111–140, 1973.
Gille, S. T.: Warming of the Southern Ocean since the 1950s. Science, 295, 1275–1277, 2002.
Gordon, A. L.: Weddell deep water variability, J. Mar. Res., 40(Suppl.), 199–217, 1982.
Gordon, A. L., Orsi, A. H., Muench, R., Huber, B. A., Zambianchi, E., and Visbeck, M.: Western Ross Sea continental slope gravity currents, Deep-Sea Res. Pt. II, 56, 796–817, doi:10.1016/j.dsr2.2008.10.037, 2009.
Gordon, A. L., Huber, B. A., Mckee, D., and Visbeck, M.: A seasonal cycle in the export of bottom water from the Weddell Sea, Nat. Geosci., 3, 551–556, 2010.
Gouretski, V. V. and Jancke, K.: A new hydrographic data set for the South Pacific: synthesis of WOCE and historical data. WHP SAC Technical Report No. 2, WOCE Report No. 143/96 (unpublished manuscript), WHP Special Analysis Centre, 1996.

Hall, A. and Visbeck, M.: Synchronous variability in the Southern Hemisphere atmosphere, sea ice, and ocean resulting from the annular mode, J. Climate, 15, 3043–3057, 2002.
Hellmer, H. H., Kauker, F., and Timmermann, R.: Weddell Sea anomalies: Excitation, propagation, and possible consequences, Geophys. Res. Lett., 36, L12605, doi:10.1029/2009GL038407, 2009.
Hellmer, H. H., Huhn, O., Gomis, D., and Timmermann, R.: On the freshening of the northwestern Weddell Sea continental shelf, Ocean Sci., 7, 305–316, doi:10.5194/os-7-305-2011, 2011.
Hoppema, M., Dehairs, F., Navez, J., Monnin, C., Jeandel, C., Fahrbach, E., and de Baar, H. J. W.: Distribution of barium in the Weddell Gyre: impact of circulation and biogeochemical processes, Mar. Chem., 122, 118–129, doi:10.1016/j.marchem.2010.07.005, 2010.
Huhn, O., Hellmer, H. H., Rhein, M., Rodehacke, C., Roether, W., Schodlok, M. P., and Schröder, M.: Evidence of deep- and bottom-water formation in the Western Weddell Sea, Deep-Sea Res. Pt. II, 55, 1098–1116, 2008.
Jackett, S. S. and McDougall, T. J.: A neutral density variable for the world's oceans, J. Phys. Oceanogr., 27, 237–263, 1997.
Jacobs, S. S. and Comiso, J. C.: Sea Ice and Oceanic Processes on the Ross Sea Continental Shelf, J. Geophys. Res., 94, 18195–18211, 1989.
Jacobs, S. S. and Giulivi, C. F.: Large Multidecadal Salinity Trends near the Pacific–Antarctic Continental Margin, J. Climate, 23, 4508–4524, doi:10.1175/2010JCLI3284.1, 2010.
Jacobs, S. S., Guilivi, C. F., and Mele, P.: Freshening of the Ross Sea during the late 20th century, Science, 297, 386–389, 2002.
Johnson, G.: Recent decadal warming and freshening of Antarctic-derived abyssal waters, IOP C. Ser. Earth Env., 6, 032006, doi:10.1088/1755-1307/6/3/032006, 2009.
Kalnay, E., Kanamitsu, M., Kistler, R., Collins, W., Deaven, D., Gandin, L., Iredell, M., Saha, S., White, G., Wollen, J., Zhu, Y., Letman, A., Reynolds, R., Chelliah, M., Ebisuzaki, W., Higgins, W., Janowiak, J., Moo, K. C., Ropelewski, C., Wang, J., Jenne, R., and Josepf, D.:: The NCEP/NCAR 40-year reanalysis project, B. Am. Meteorol. Soc., 77(3), 437–471, 1996.
Kerr, R., Mata, M. M. and Garcia, C. A. E.: On the temporal variability of the Weddell Sea Deep Water Masses, Antarct. Sci., 21(4), 383–400. doi:10.1017/S0954102009001990, 2009a.
Kerr, R., Wainer, I., and Mata, M. M.: Representation of the Weddell Sea Deep Water Masses in the ocean component of the NCAR-CCSM model, Antarct. Sci., 21(3), 301–312.

Discussion Paper | Discussion Paper | Discussion Paper | Discussion Paper |

doi:10.1017/S0954102009001825, 2009b.
Kerr, R., Wainer, I., Mata, M. M., and Garcia, C. A. E.: Quantifying Antarctic deep waters in SODA reanalysis product, Pesquisa Antártica Brasileira, 5, accepted, 2011.
Large, W. G., Danabasoglu, G., Doney, S. C., and McWillians, J. C.: Sensitivity to surface forcing and boundary layer mixing in a global ocean model: annual-mean climatology, J. Phys. Oceanogr., 27(11), 2418–2447, 1997.
McKee, D. C., Yuan, X., Gordon, A. L., Huber, B. A., and Dong, Z.: Climate impact on interannual variability of Weddell Sea Bottom Water, J. Geophys. Res., 116, C05020, doi:10.1029/2010JC006484, 2011.
Mensch, M., Simom, A., and Bayer, R.: Tritium and CFC input functions for the Weddell Sea, J. Geophys. Res., 103, 15923–15937, 1998.
Muench, R. D. and Gordon, A. L.: Circulation and transport of water along the Western Weddell Sea margin, J. Geophys. Res., 100, 18503–18515, 1995.
Naveira Garabato, A. C., McDonagh, E. L., Stevens, D. P., Heywood, K. J., and Sanders, R. J.: On the export of Antarctic Bottom Water from the Weddell Sea, Deep-Sea Res. Pt. II, 49, 4715–4742, 2002.
Nicholls, K. W., Østerhus, S., Makinson, K., Gammelsrød, T., and Fahrbach, E.: Ice-ocean process over the continental shelf of the Southern Weddell Sea, Antarctica: a review, Rev. Geophys., 47, RG3003, 2007RG000250, 2009.
Orsi, A. H. and Whitworth, T.: Hydrographic Atlas of the World Ocean Circulation Experiment (WOCE) Volume 1: Southern Ocean, edited by: Sparrow, M., Chapman, P., and Gould, J., Department of Oceanography, Texas A&M University, College Station, Texas, USA Series, 2007.
Orsi, A. H., Nowlin, W. D., and Whitworth, T.: On the circulation and stratification of the Weddell Gyre, Deep-Sea Res. Pt. I, 40, 169–303, 1993.
Orsi, A. H., Johnson, G. C., and Bullister, J. L.: Circulation, mixing, and production of Antarctic Bottom Water, Prog. Oceanogr., 43, 55–109, 1999.
Ozaki, H., Obata, H., Naganobu, M., and Gamo, T.: Long-Term Bottom Water Warming in the North Ross Sea, J. Oceanogr., 65, 235–244, 2009.
Reid, J. L.: On the total geostrophic circulation of the Pacific Ocean: flow patterns, tracers, and transports, Prog. Oceanogr., 39, 263–352, 1997.
Renner, A. H. H., Heywood, K. J., and Thorpe, S. E.: Validation of global ocean models in the Weddell Sea, Ocean Model., 30(1), 1–15 doi:10.1016/j.ocemod.2009.05.007, 2009.

Rignot, E. and Jacobs, S. S.: Rapid bottom melting widespread near Antarctic ice sheet grounding lines, Science, 296, 2020–2023, 2002.
Rintoul, S.: Rapid freshening of Antarctic Bottom Water formed in the Indian and Pacific oceans, Geophys. Res. Lett., 34, LI06606, doi:10.1029/2006GL028550, 2007.
Robertson, R., Visbeck, M., Gordon, A. L., and Fahrbach, E.: Longterm temperature trends in the deep waters of the Weddell Sea, Deep-Sea Res. Pt. II, 49, 4791–4806, 2002.
Schlosser, P., Bullister, J. L., and Bayer, R.: Studies of deep water formation and circulation in the Weddell Sea using natural and anthropogenic tracers, Mar. Chem., 35, 97–122, 1991.
Smedsrud, L. H.: Warming of the deep water in the Weddell Sea along the Greenwich meridian: 1977–2001. Deep-Sea Res. Pt. I, 52, 241–258, 2005.
Smith, W. H. F. and Sandwell, D. T.: Global seafloor topography from satellite altimetry and ship depth soundings, Science, 277, 1957–1962, 1997.
Thompson, A. F. and Heywood, K. J.: Frontal structure and transport in the Northwestern Weddell Sea, Deep-Sea Res. Pt. I, 55, 1229–1251, doi:10.1016/j.dsr.2008.06.001, 2008.
Trumbore, S., Jacobs, S. S., and Smethie Jr., W.: Chlorofluorocarbon evidence for rapid ventilation of the Ross Sea, Deep-Sea Res., 38(7), 845–870, 1991.
Venegas, S. A. and Drinkwater, M. R.: Sea ice, atmosphere and upper ocean variability in the Weddell Sea, Antarctica, J. Geophys. Res., 106(C8), 16747–16765, 2001.
Whitworth III, T. and Orsi, A. H.: Antarctic Bottom Water production and export by tides in the Ross Sea, Geophys. Res. Lett., 33, L12609, doi:10.1029/2006GL026357, 2006.
Whitworth III, T., Orsi, A. H., Kim, S.-J., Nowlin Jr., W. D., and Locarnini, R. A.: Water masses and mixing near the Antarctic Slope Front, in: Ocean, Ice, and Atmosphere: Interactions at the Antarctic Continental Margin, edited by: Jacobs, S. S. and Weiss, R. F., Antarctic Research Series, 75, Washington DC, AGU, 1–27, 1998.

OSD
8, 1657–1694, 2011

On the export of dense water from the Weddell and Ross Seas

R. Kerr et al.

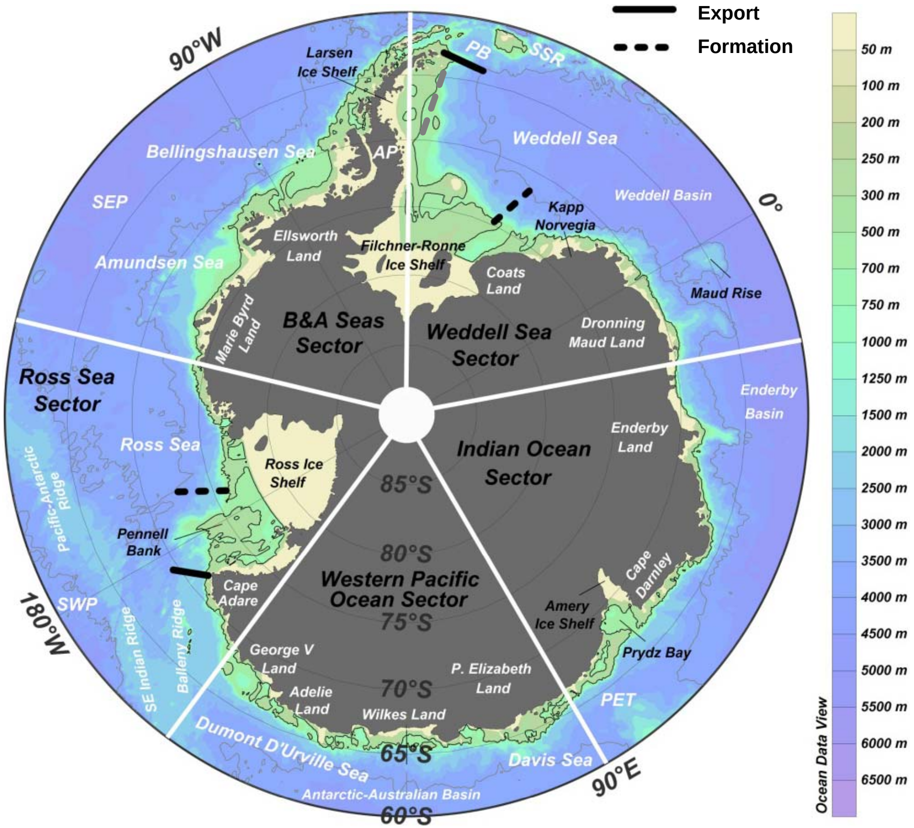

Fig. 1. Southern Ocean sectors. The black thick (dashed) lines are Weddell and Ross Seas export (formation) cross-shelf sections. The black (grey) thin line is the 500 m (4000 m) isobaths. The grey thick line along the 500 m isobaths is the Northwestern Weddell Sea formation section. Antarctic Peninsula = AP, Powell Basin = PB, Princess Elizabeth Though = PET, South Scotia Ridge = SSR, and Southeastern (Southwestern) Pacific Basin = SEP (SWP).

OSD
8, 1657–1694, 2011

On the export of dense water from the Weddell and Ross Seas

R. Kerr et al.

Title Page
Abstract | Introduction
Conclusions | References
Tables | Figures
◀▮ | ▶▮
◀ | ▶
Back | Close
Full Screen / Esc
Printer-friendly Version
Interactive Discussion

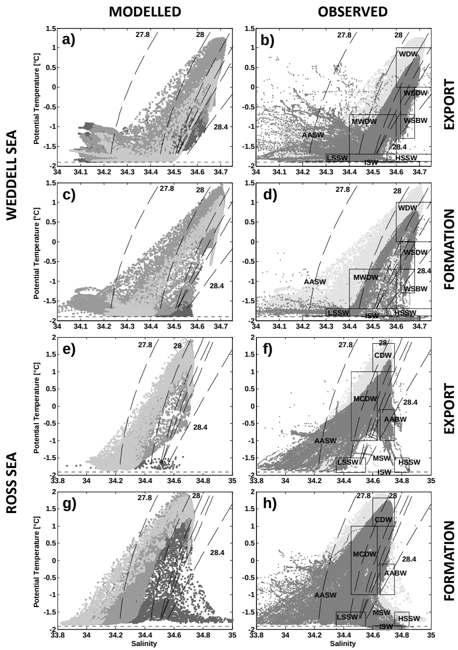

Fig. 2. (a–d) Weddell and **(e–h)** Ross Seas OCCAM monthly average (left column) and (right column) observed potential temperature/salinity (θ/S) diagrams. **(a, b, e, f)** Export and **(c, d, g, h)** formation sections. Colours in the left column indicate: continental shelf (dark grey), continental slope (grey), and deep ocean (light grey). Colours in the right column indicate: OCCAM simulation (light grey) and observations (dark grey). Dashed lines are neutral densities of 27.8, 28, 28.1, 28.2, 28.26, 28.40 kg m^{-3}, respectively. The dotted line is the freezing point temperature. See the text for water masses definitions. Antarctic Surface Water = AASW, High Salinity Shelf Water = HSSW, Ice Shelf Water = ISW, Low Salinity Shelf Water = LSSW, Circumpolar Deep Water = CDW, Warm Deep Water = WDW, Modified CDW = MCDW, Modified WDW = MWDW, Modified Shelf Water = MSW, Antarctic Bottom Water = AABW, Weddell Sea Deep Water =WSDW, and Weddell Sea Bottom Water = WSBW.

OSD
8, 1657–1694, 2011

On the export of dense water from the Weddell and Ross Seas

R. Kerr et al.

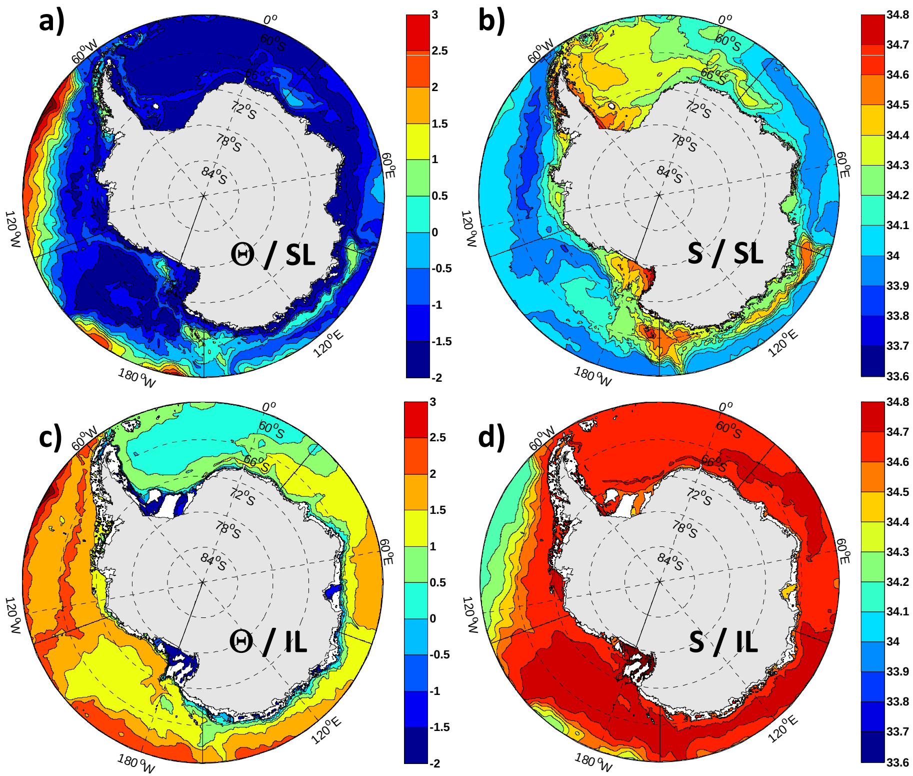

Fig. 3. OCCAM average field at (**a** and **b**) shelf/surface layer (SL) and (**c** and **d**) intermediate layer (IL) of (left) potential temperature (θ) in °C and (right) salinity (S).

OSD
8, 1657–1694, 2011

On the export of dense water from the Weddell and Ross Seas

R. Kerr et al.

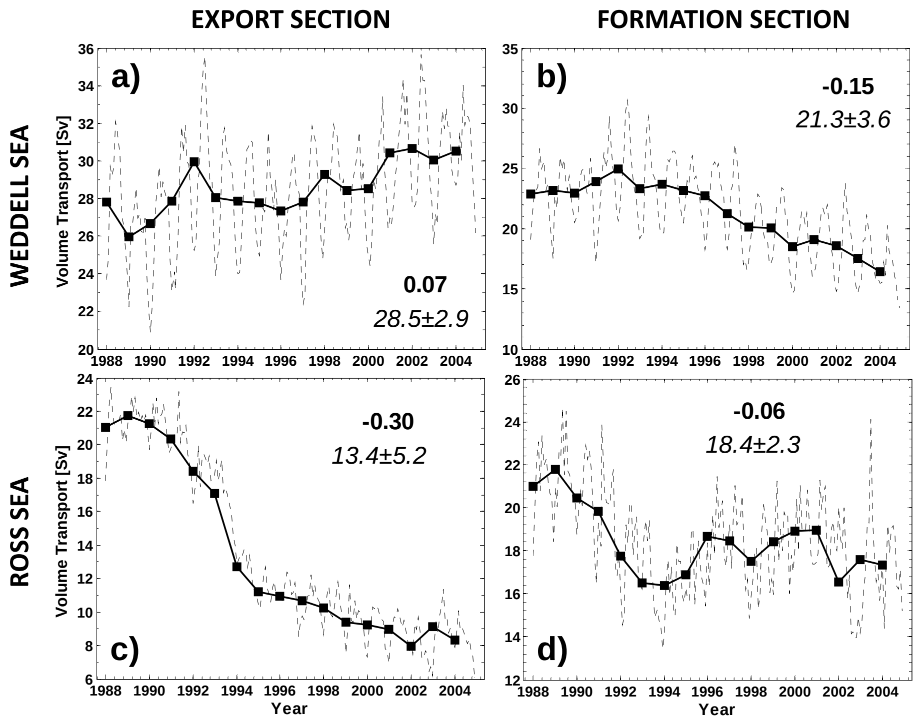

Fig. 4. Monthly (dashed line) and annual (full line) average of OCCAM full-depth cumulative volume transport for (**a** and **b**) Weddell and (**c** and **d**) Ross Seas (**a** and **c**) export and (**b** and **d**) formation sections. The bold and italic annotations show respectively the decadal linear trend (Sv decade^{-1}) and the average and standard deviation for the entire period.

OSD
8, 1657–1694, 2011

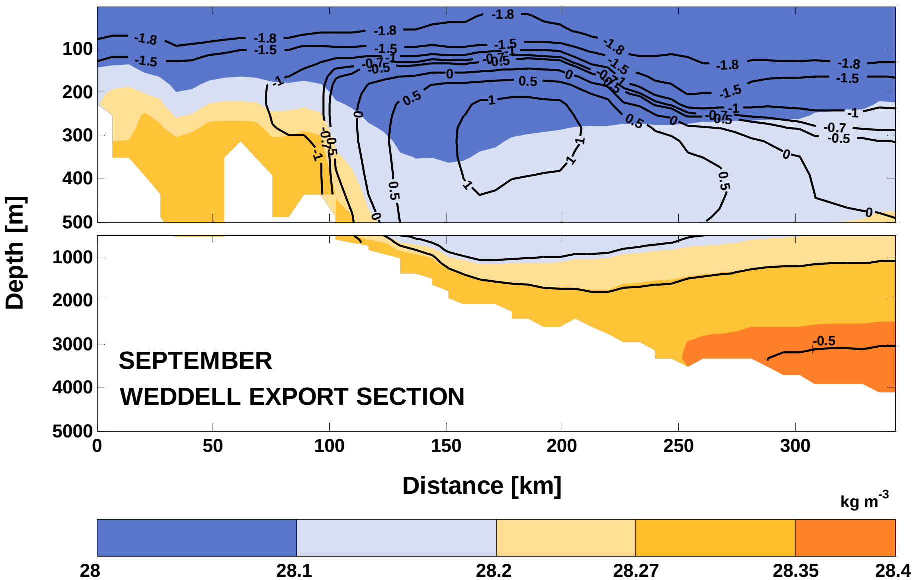

Fig. 5. Weddell Sea export section fields of (colour) neutral density in kg m^{-3} and (isolines) potential temperature in $^{\circ}$C of OCCAM September climatology.

OSD
8, 1657–1694, 2011

On the export of dense water from the Weddell and Ross Seas

R. Kerr et al.

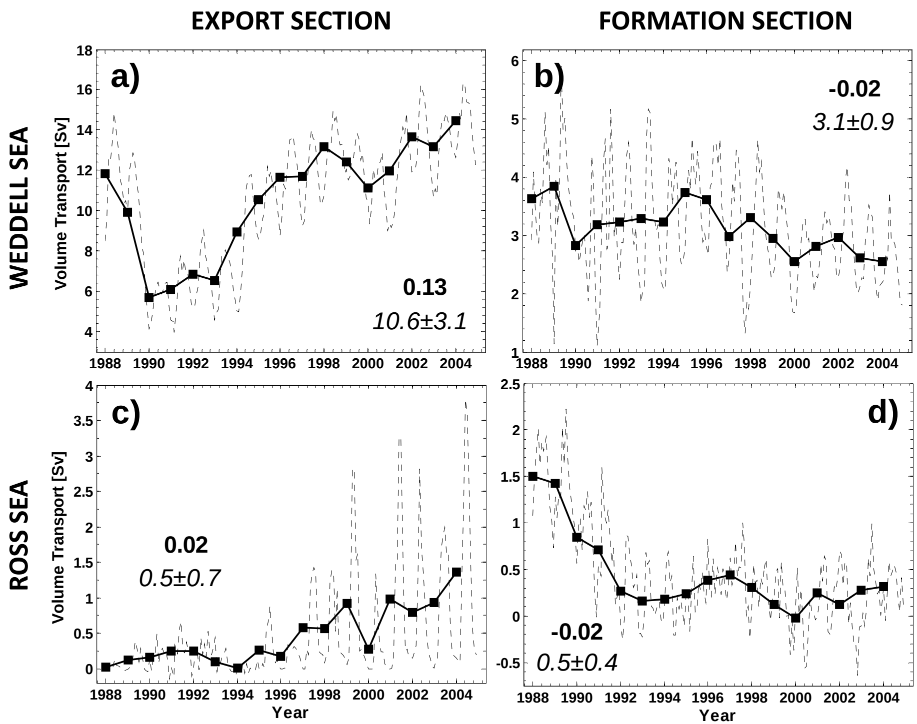

Fig. 6. Monthly (dashed line) and annual (full line) average of OCCAM simulated bottom layer volume transport for (**a** and **b**) Weddell and (**c** and **d**) Ross Seas (**a** and **c**) export and (**b** and **d**) formation sections. The bold and italic annotations show respectively the decadal linear trend (Sv decade^{-1}) and the average and standard deviation for the entire period.

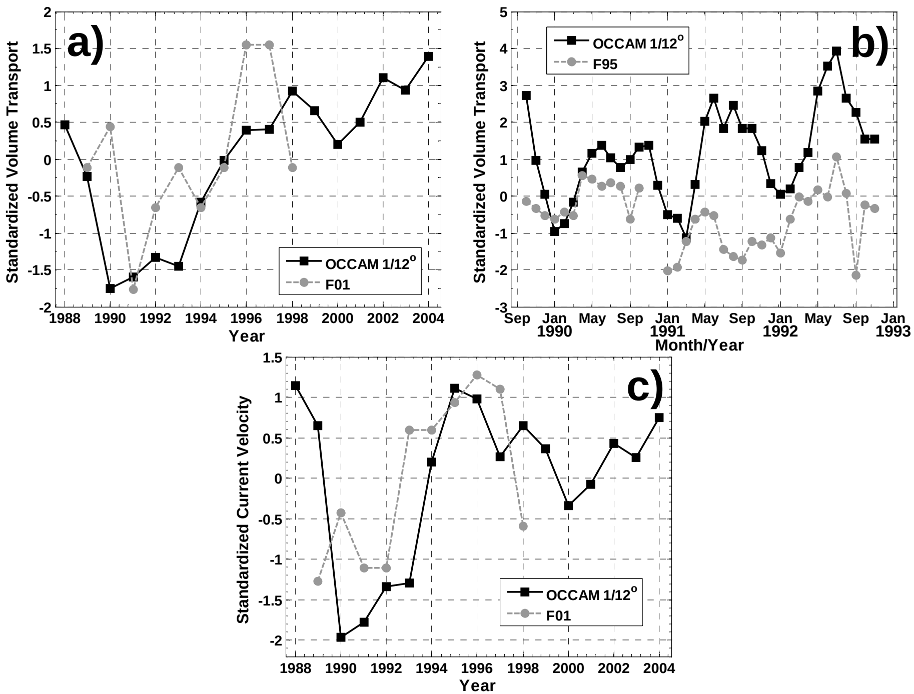

Fig. 7. Weddell Sea export section standardized bottom volume transport **(a)** annual and **(b)** monthly average simulated by OCCAM (black line) and reported (grey line) by Fahrbach et al. (1995) = F95 and Fahrbach et al. (2001) = F01. **(c)** Same as described above, but for bottom layer current velocity perpendicular to the bathymetry. The units are point-wise normalized and represent the number of standard deviations from the overall mean.

OSD
8, 1657–1694, 2011

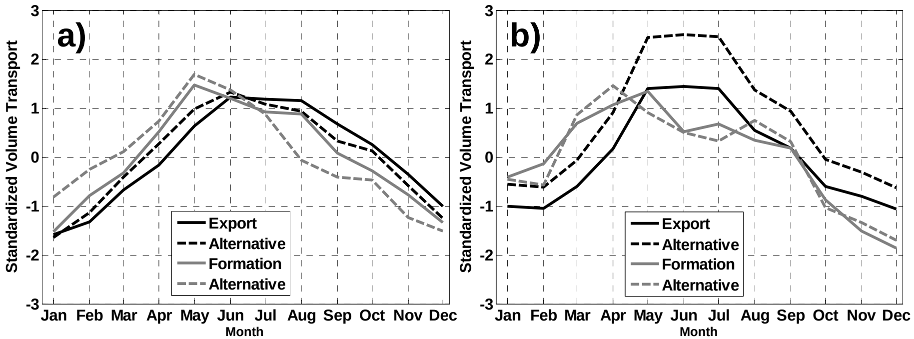

Fig. 8. Standardized annual cycle of the bottom layer volume transport for the entire OCCAM simulation in **(a)** Weddell and **(b)** Ross Seas. The thick lines show the sections used in this study while the dashed lines show the alternative sections selected near each section. The units are point-wise normalized and represent the number of standard deviations from the overall mean.

OSD

8, 1657–1694, 2011

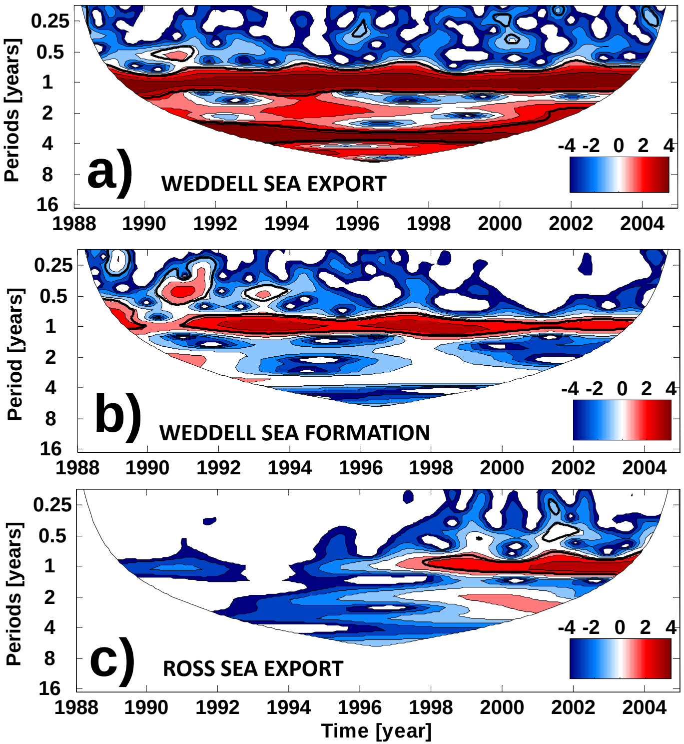

Fig. 9. The wavelet power spectrum of **(a)** Weddell Sea export, **(b)** Weddell Sea formation, **(c)** and Ross Sea export volume transport anomaly using the Morlet wavelet. The white area is the cone of influence, where zero padding has reduced the variance. The black thick contour encloses regions where confidence levels were greater than 90 % for a red-noise process with a lag-1 coefficient of 0.72. The units (colorbar) are the energy in $\log_2$ form.

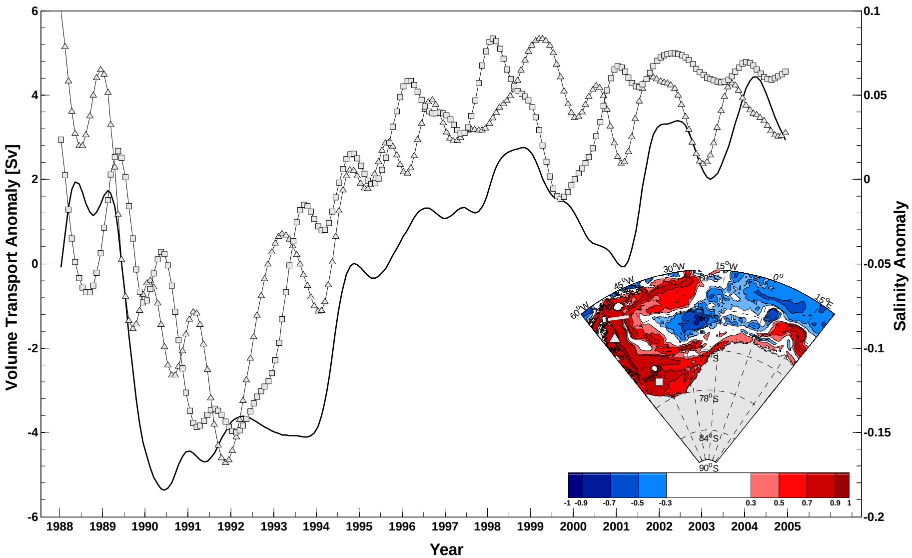

Fig. 10. Bottom volume transport anomaly time series (Sv; black line) of Weddell export section (inset figure – grey line) and salinity anomaly time series at the locations marked by square and triangle symbols in the inset figure (see caption of Fig. 11), which shows the high degree of correlation between the time series.

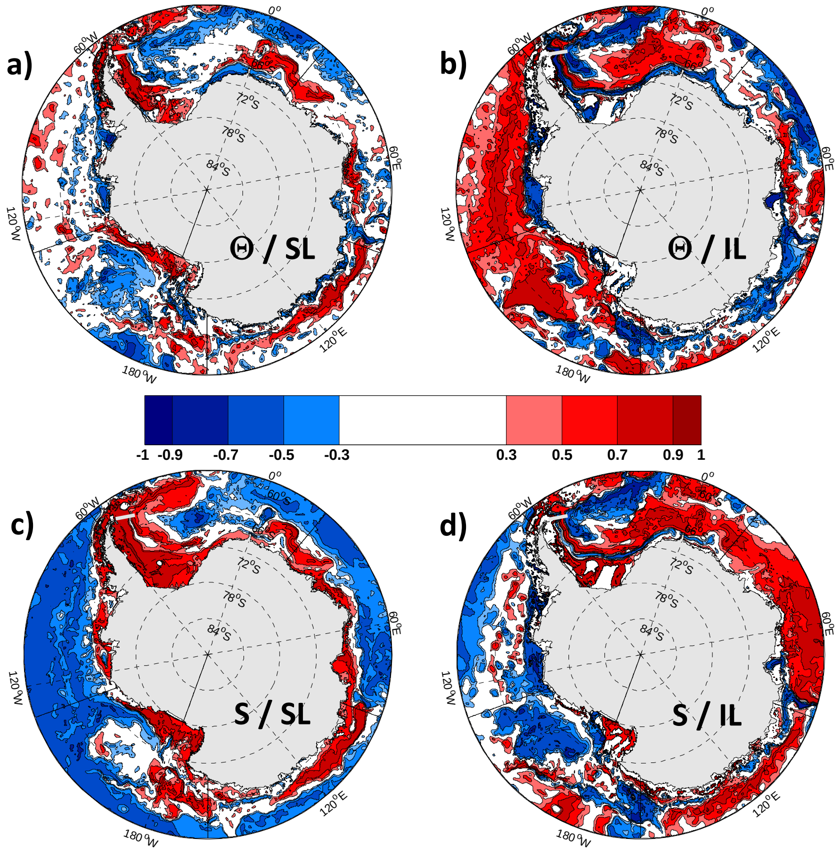

Fig. 11. Cross-correlation maps between model monthly mean bottom layer volume transport at Weddell export section (grey line) onto (**a** and **b**) potential temperature and (**c** and **d**) salinity at (**a** and **c**) SL depth and (**b** and **d**) IL depth. All correlations are calculated for lag-0. Only correlation coefficients at 95 % significance level are shown.

OSD
8, 1657–1694, 2011

On the export of dense water from the Weddell and Ross Seas

R. Kerr et al.

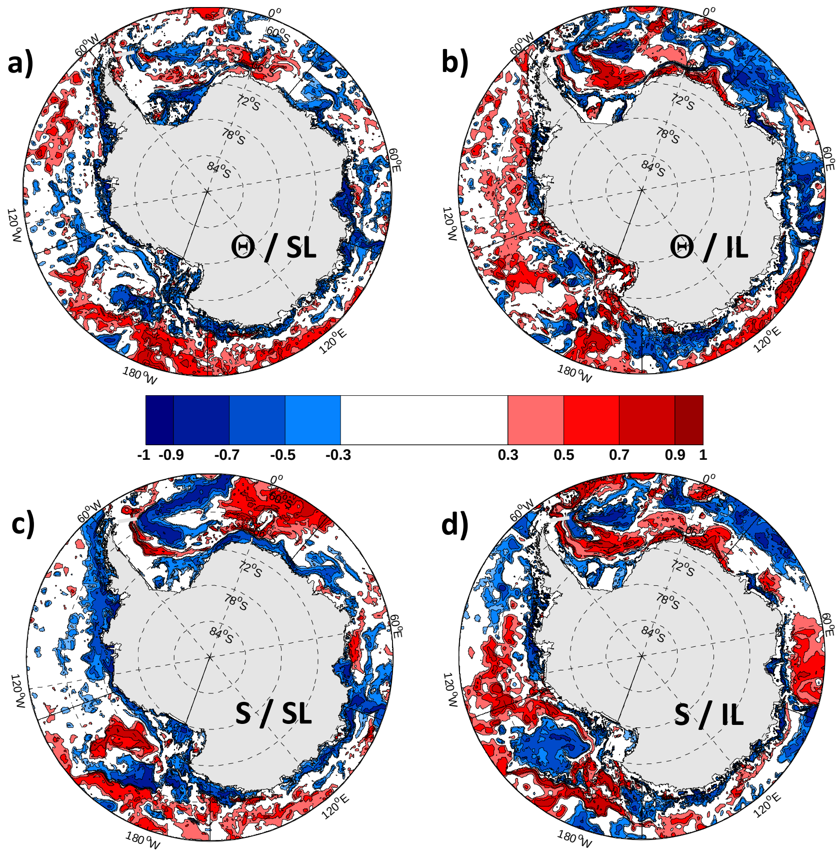

Fig. 12. Same as Fig. 11, but for correlations calculated for lag-5.

OSD
8, 1657–1694, 2011

On the export of dense water from the Weddell and Ross Seas

R. Kerr et al.

Title Page
Abstract Introduction
Conclusions References
Tables Figures
◀◀ ▶▶
◀ ▶
Back Close
Full Screen / Esc
Printer-friendly Version
Interactive Discussion

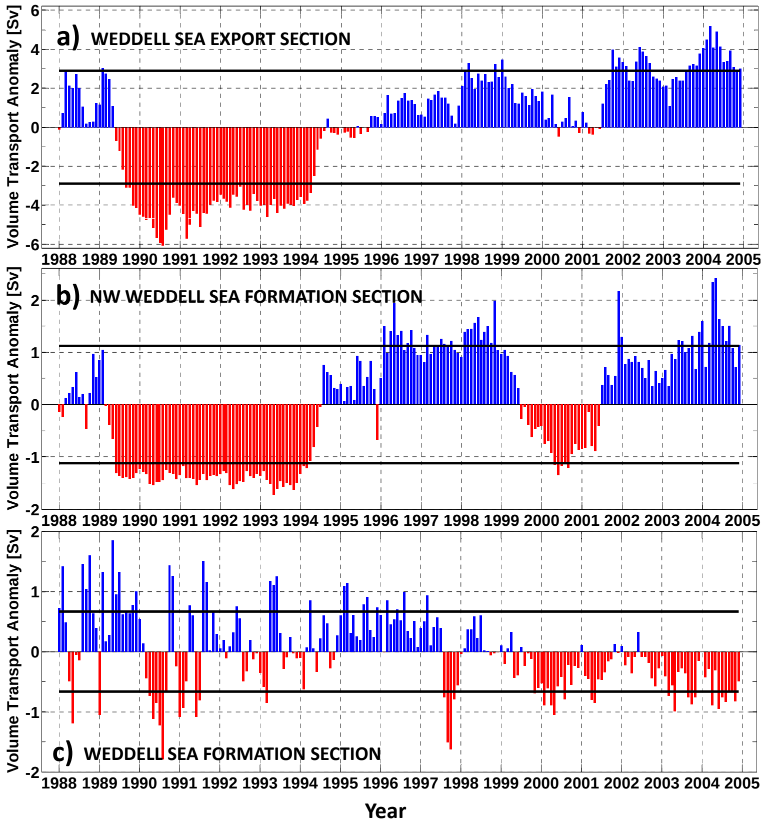

Fig. 13. Volume transport anomaly time series (Sv) in Weddell Sea **(a)** export zone and **(b)** northwestern and **(c)** southern formation regions. The black thick lines indicate one standard deviation.

OSD
8, 1657–1694, 2011

On the export of dense water from the Weddell and Ross Seas

R. Kerr et al.

Title Page
Abstract | Introduction
Conclusions | References
Tables | Figures
◂ | ▸
Back | Close
Full Screen / Esc
Printer-friendly Version
Interactive Discussion

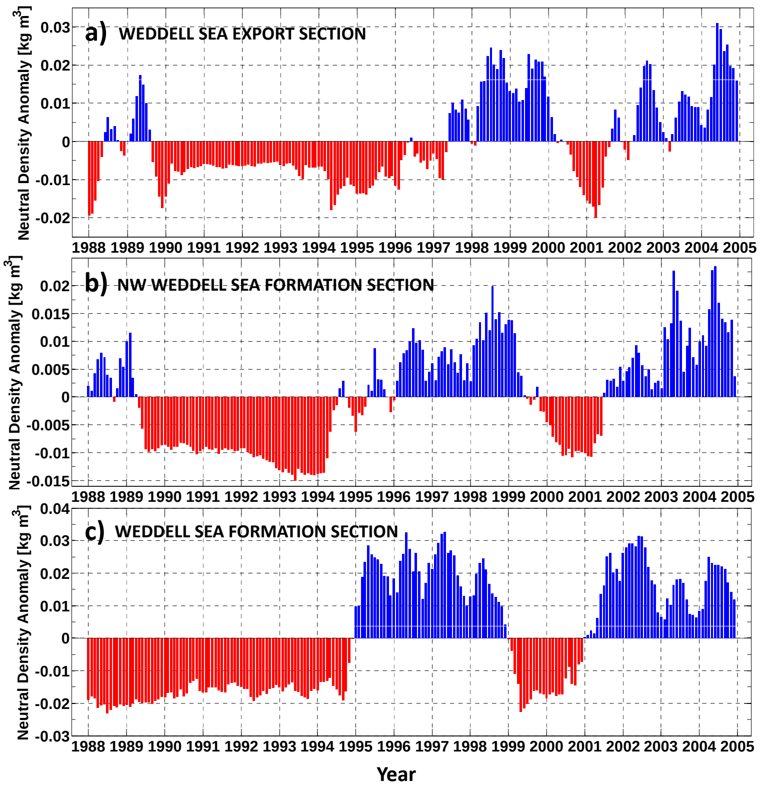

Fig. 14. Neutral density anomaly time series (kg m^{-3}) in Weddell Sea **(a)** export zone and **(b)** northwestern and **(c)** southern formation regions.

OSD
8, 1657–1694, 2011

On the export of dense water from the Weddell and Ross Seas

R. Kerr et al.